論文 / 著書情報
Article / Book Information

Title	A successive LP approach with C-VaR type constraints for IMRT optimization
Authors	Shogo Kishimoto, Makoto Yamashita
Citation	Operations Research for Health Care, Volume 17, pp. 55-64
Pub. date	2018, 6
DOI	http://dx.doi.org/10.1016/j.orhc.2017.09.007
Creative Commons	See next page.
Note	This file is author (final) version.

License

A Successive LP Approach with C-VaR Type Constraints for IMRT Optimization

Shogo Kishimoto [1] and Makoto Yamashita [2]

Submitted: December 5, 2016. Revised: July 14, 2017 and September 20, 2017.

Abstract:

In this paper, we propose a successive linear programming (LP) approach for an intensity-modulated radiotherapy treatment (IMRT) optimization. The use of IMRT enables to control the beam intensities accurately and gives more flexibility for cancer treatment plans, but finding a feasible plan that satisfies all dose-volume constraints (DVCs) requires expensive computation cost. Romeijn et al. [Physics in Medicine and Biology, 48(21):3521, 2003] replaced the DVCs with C-VaR (conditional Value-at-Risk) type constraints, and successfully reduced this computation cost. However, the feasible region of the LP problem was small compared to the original DVCs, therefore, their approach often failed to find a feasible plan even when the DVCs were not so stringent.

In the proposed method, we integrate the C-VaR type constraints with a successive LP approach. Exploiting the solution of LP problems, we automatically detect outliers and remove them from the domain of the C-VaR type constraints. This reduces the sensitivity of the C-VaR type constraints to outliers, therefore, we can search feasible plans in a wider region than the C-VaR type constraints. We give a mathematical proof that if the optimal value of an LP problem in the proposed method is non-positive, the corresponding optimal solution satisfies all the DVCs. From a numerical experiment on test data sets, we observed that the proposed method found feasible solutions more appropriately than existing successive LP approaches. Moreover, the proposed method required fewer LP problems, and this was reflected in a short computation time.

Keywords: Intensity-modulated radiotherapy treatment, Fluence map optimization, Linear programming, Condtional Value-at-Risk

1 Introduction

In many countries, cancer is considered to be one of the principal causes of death. In Japan, it was reported in [9] that the fatalities number rose to 350 thousand people and 800 thousand people were newly diagnosed as cancer in the year 2010. Prevalent types of cancer treatment include chemotherapy, surgery, and radiation therapy. An investigation conducted by Ministry of Health, Labor and Welfare of Japan [11] reported that their percentages are 81%, 72%, and 32%, respectively (the numbers include combinations of treatment types). The National Cancer Institute reported that a half of the cancer patients receive radiation therapy during their treatment [13]. Among radiation therapy, intensity-modulated radiotherapy treatment (IMRT) has brought a remarkable flexibility in dose irradiated from the beams. The computation of IMRT

[1] Department of Mathematical and Computing Sciences, Tokyo Institute of Technology, 2-12-1-W8-29 Ookayama, Meguro-ku, Tokyo 152-8552, Japan (kishimoto.s.ac@m.titech.ac.jp).

[2] Department of Mathematical and Computing Science, Tokyo Institute of Technology, 2-12-1-W8-29 Ookayama, Meguro-ku, Tokyo 152-8552, Japan (Makoto.Yamashita@is.titech.ac.jp). His research was partially supported by JSPS KAKENHI (Grant Number: 15K00032).

planning involves several optimization aspects. For instance, the handbook [14] discusses various aspects on IMRT from the viewpoints of optimization in Chapters 4 and 5.

A difficulty raised in IMRT planning is that not only malignant tumors but also normal tissues near the tumors receive adverse damage from the beam irradiation. Oncologists develop treatment plans for the irradiation areas and the beam intensity to reduce the damage onto the normal tissues. A key clinical criterion that measures the quality of a treatment plan is to satisfy dose-volume constraints (DVCs), which specify the lower or upper bounds on the fraction of tissues that receive a specified dose or higher. Although it is ideal to irradiate higher doses than a prescribed level to all parts of the tumors and lower doses than some threshold to the normal tissues, such an ideal treatment plan is difficult to realize when the tumors and the normal tissues are in proximity to each other. In the case DVCs are employed, a treatment plan is acceptable if the fraction of the part receiving extreme doses is within a certain range. Therefore, outliers that receive extreme doses are permitted in the framework of DVCs on the condition that the fraction of the outliers is limited.

To find a suitable treatment plan that satisfies all the DVCs, a number of approaches have been proposed based on mathematical optimization methods. In this paper, we are focused on fluence map optimization (FMO) [2, 16, 17] and an FMO problem is an optimization problem to determine the irradiation intensity of beams for given beam angles. FMO problems with DVCs formulated in mathematical optimization problems often have multiple local minimum solutions [18] and the problems are usually NP-hard [17]. To reduce the computation cost of difficult DVCs, many approach have examined approximations of DVCs. Morrill et al. [12] employed linear programming (LP) problems, and Aleman et al. [1] solved an optimization problem that minimizes the deviations from DVCs using a quadratic objective function.

One successful way to obtain good approximations of DVCs is C-VaR (conditional value-at-risk) type constraints introduced by Romeijn et al. [16]. The C-VaR type constraints impose the *average* dose in a given fraction part satisfy a given threshold, and such constraints can be described as linear constraints, therefore, the optimization problem solved in [16] is an LP problem. An advantage of the C-VaR type constraints is that irradiation intensities obtained from the LP problem always satisfy all the DVCs (This property is not clearly mentioned in [16], and we will verify it later in Lemma 2.1). The C-VaR type constraints have been discussed in several papers, for example, Chan et al. [3] applied a robust computation framework to the C-VaR type constraints for breast cancer therapy, and Mahmoudzadeh et al. [8] reduced the computation cost of the LP problems with an outer approximation. Recently, Engberg et al. [6] discussed multi-criteria optimization techniques for the FMO problems with the C-VaR type constraints.

However, the feasible region of the LP problem in [16] is very small compared to the original region defined by the DVCs. Since the LP problems can be solved by a polynomial-time algorithms while the FMO problems themselves are NP-hard, we cannot completely remove the gap between the C-VaR type constraints and the DVCs. In particular, a few parts of the body receive extremely high doses, and such outliers seriously affect the average dose in the C-VaR type constraints. This effect makes it very hard to find a feasible plan that satisfies all the DVCs. In fact, the approach in [16] was unable to find the beam intensities for some test instances of Task Group (TG) 119 report by the American Association of Physicists in Medicine (AAPM) [7]. The papers above [3, 6, 8] that utilized the C-VaR type constraints did not focus on the acute effect of the outliers onto the C-VaR type constraints. Even though the use of the robust optimization framework in [3] might relieve this serious effect, the set of uncertainty for the C-VaR type constraints must be fixed in advance, hence the outliers cannot be resolved automatically.

On the other hand, Merrit et al. [10] proposed a successive LP approach to overcome the outliers in FMO problems. In determining the beam intensities, their approach detected the outliers based on the information of a dual LP problem, and relaxed the dose thresholds. This

mechanism gradually relieved the effect from the outliers. However, such a mechanism has not been considered with the C-VaR constraints before.

In this paper, we propose a successive LP approach that employs the C-VaR type constraints. We first relax the C-VaR type constraints so that each LP problem always has an optimal solution. Then, we detect the outliers from the optimal solution of the LP problem, and delete them from the domain of the C-VaR type constraints in the next LP problems. This automatic adjustment of the outliers enables to search a feasible plan in a wider region than the successive approach of Merrit at al. [10].

We will show mathematically that if the objective values of the successive LP problems become non-positive, the proposed method outputs beam intensities that satisfy all the DVCs. In addition, the sequence of the objective values of the successive LP problems is non-increasing. This property implies that we can generate a sequence of the solutions that approaches to the DVCs. Since our optimization problems are still LP problems, the computation cost is still low compared to the original DVCs. We conducted a numerical test to evaluate the performance of the proposed method. For test instances included in TG 119, the proposed approach found beam intensities that satisfied the DVCs within a short computation time. In addition, the solution of our approach satisfied the DVCs more appropriately than the approach of Merrit et al.

The rest of this paper is organized as follows. In Section 2, we first give precise definitions and notation on DVCs and briefly discuss the approaches of Merrit at al. and Romeijn et al. In Section 3, we describe the details on the proposed method and, in Theorem 3.2, we give a proof of its mathematical properties that are favorable for the FMO computation. Section 4 reports the numerical results on the TG 119 test instances, and in Section 5, we will discuss several aspects of the proposed methods. Finally, we will provide a conclusion in Section 6.

2 Preliminaries and Existing Methods

In the following, we use $|S|$ to denote the cardinality of a set S. A nonnegative part of a number x will be denoted by $(x)^+ := \max\{x, 0\}$.

2.1 Preliminaries

To apply numerical computation, intended organs (or structures) and radiation beams are discretized into *voxels* and *beamlets*, respectively. Let S be the set of the structures, and for each structure $s \in S$, we use V_s to denote the voxel set of s. Without loss of generality, we assume $|V_s| > 0$ throughout of this paper. The set of beamlet is denoted by B.

It is often assumed the dose that the ith voxel in the sth structure receives can be expressed in $z_{si} = \sum_{j \in B} D_{sij} x_j$. Here, x_j is the intensity of the jth beamlet. The element D_{sij} is the (i, j)th element of a fluence matrix $\boldsymbol{D}_s \in \mathbb{R}^{|V_s| \times |B|}$, and we assume that the fluence matrix is given in the material below.

We can identify a DVC by a structure s and a fractional parameter $\alpha \in (0, 1)$. The DVCs are classified into the two types, the upper and lower DVCs;

(upper) The fraction of the voxels in the structure s that receive at least U_s^α Gy is bounded α from above; In a mathematical form, $\frac{|\{i \in V_s | z_{si} > U_s^\alpha\}|}{|V_s|} \leq \alpha$.

(lower) The fraction of the voxels in the structure s that receive at least L_s^α Gy is bounded α from below; In a mathematical form, $\frac{|\{i \in V_s | z_{si} > L_s^\alpha\}|}{|V_s|} \geq \alpha$.

As an example, let us impose three DVCs to a planning target volume (PTV); $L_{\mathrm{PTV}}^{0.99} = 46.5$, $L_{\mathrm{PTV}}^{0.9} = 50.0$, and $U_{\mathrm{PTV}}^{0.2} = 55.0$. In this case, 99% of PTV must receive at least 46.5 Gy. Furthermore, 90% of PTV should receive higher doses than 50.0 Gy. At the same time, we should avoid

extremely strong intensity and this is expressed by the upper constraint of $U^{0.2}_{\mathrm{PTV}}$, that is, at most 20% voxels can exceed 55.0 Gy in PTV.

In the following discussion, we will use $\underline{A}_s$ and $\overline{A}_s$ to denote the set of the fractions used in the lower and upper DVCs for the structure s, respectively. For each $\alpha \in \overline{A}_s$, we associate the upper DVC whose threshold is U^{α}_s Gy. Similar notation is applicable to $\alpha \in \underline{A}_s$ for the lower DVC with L^{α}_s Gy. In the DVC example above, we have $\underline{A}_{PTV} = \{0.9, 0.99\}$ and $\overline{A}_{PTV} = \{0.2\}$. Without loss of generality, we assume that $\underline{A}_s \subset (0, 1)$ and $\overline{A}_s \subset (0, 1)$. For the specific fractional cases corresponding to $\alpha = 0$ or $\alpha = 1$, we denote the upper or lower bounds by U_s and L_s, respectively. When these thresholds are used, *each* voxel in the structure s is required to receive the dose between L_s and U_s.

Here, we also introduce dose-volume histograms (DVHs), since we will use DVHs to describe a key concept of the proposed method in Section 3. Figure 1 shows an example of DVHs, in which the blue line is a histograms for PTV and the other lines are for Cord, Lt Parotid and Rt Parotid. The horizontal axis is a dose and the vertical axis is the fraction of the structure. The PTV histogram passes the point (50 Gy, 90%) and this indicates that 90% voxels in PTV receive at least 50 Gy, therefore, this histogram satisfies $L^{0.90}_{\mathrm{PTV}} = 50$.

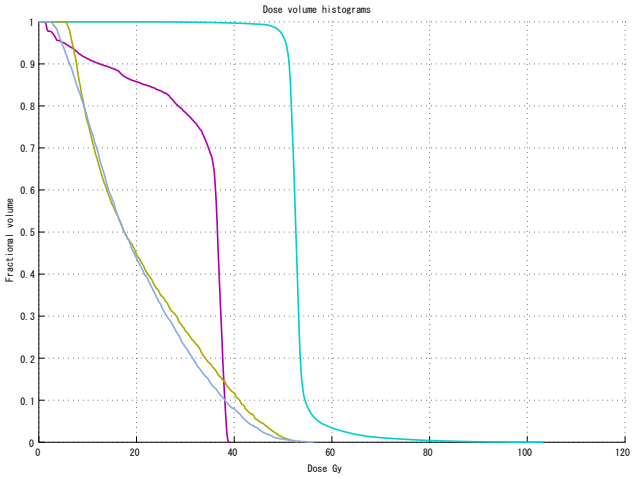

Figure 1: An example of dose-volume histograms for PTV, Cord, Lt Parotid and Rt Parotid.

Using these notations, an FMO problem to find the beamlet intensities that satisfy all the DVCs can be formulated as a mathematical problem. In particular, if we are allowed to use mixed-integer programming problems, one of the essential tasks in the FMO computation is to

find a solution of the feasible set $\mathcal{F}$ defined by

$$
\begin{array}{rlll}
\mathcal{F} := & \{\boldsymbol{x} \in \mathbb{R}^{|B|} & : & \sum_{j=1}^{|B|} D_{sij} x_j = z_{si} \quad \text{for } i = 1, \ldots, |V_s|; s = 1, \ldots, |S| \\
& & & L_s \leq z_{si} \leq U_s \quad \text{for } i = 1, \ldots, |V_s|; s = 1, \ldots, |S| \\
& & & z_{si} \geq 0 \quad \text{for } i = 1, \ldots, |V_s|; s = 1, \ldots, |S| \\
& & & z_{si} \geq L_s^{\alpha} \underline{b}_{si}^{\alpha} \quad \text{for } i = 1, \ldots, |V_s|; \alpha \in \underline{A}_s; s = 1, \ldots, |S| \\
& & & \underline{b}_{si}^{\alpha} \in \{0, 1\} \quad \text{for } i = 1, \ldots, |V_s|; \alpha \in \underline{A}_s; s = 1, \ldots, |S| \\
& & & \sum_{i=1}^{|V_s|} \underline{b}_{si}^{\alpha} \geq \alpha |V_s| \quad \text{for } \alpha \in \underline{A}_s; s = 1, \ldots, |S| \\
& & & z_{si} \leq U_s^{\alpha} + M \overline{b}_{si}^{\alpha} \quad \text{for } i = 1, \ldots, |V_s|; \alpha \in \overline{A}_s; s = 1, \ldots, |S| \\
& & & \overline{b}_{si}^{\alpha} \in \{0, 1\} \quad \text{for } i = 1, \ldots, |V_s|; \alpha \in \overline{A}_s; s = 1, \ldots, |S| \\
& & & \sum_{i=1}^{|V_s|} \overline{b}_{si}^{\alpha} \leq \alpha |V_s| \quad \text{for } \alpha \in \overline{A}_s; s = 1, \ldots, |S| \\
& & & x_j \geq 0 \quad \text{for } j = 1, \ldots, |B| \quad \}.
\end{array}
\tag{1}
$$

In this definition, M is a constant number large enough (so-called big-M). To express the fraction of the partial volume, the binary variables $\underline{b}_{si}^{\alpha}$ and $\overline{b}_{si}^{\alpha}$ are introduced. We should remark that a single upper DVC $|\{i \in V_s | z_{si} > U_s^{\alpha}\}| \leq \alpha |V_s|$ is imposed by a combination of $z_{si} \leq U_s^{\alpha} + M \overline{b}_{si}^{\alpha}$, $\overline{b}_{si}^{\alpha} \in \{0, 1\}$ and $\sum_{i=1}^{|V_s|} \overline{b}_{si}^{\alpha} \leq \alpha |V_s|$. The number of voxels exceeds thousands in practical situations, hence, the number of these binary variables ($\underline{b}_{si}^{\alpha}$ and $\overline{b}_{si}^{\alpha}$) are also considerably large. The set $\mathcal{F}$ embraces properties of combinatorial sets, and finding a feasible point in $\mathcal{F}$ exactly is an NP-hard task [17].

2.2 A Successive Linear Programming Method

In 2002, Merritt et al. [10] employed a successive LP approach to handle the FMO problem. Their method is referred as Method-M in the material below.

A core idea of Method-M is to solve LP problems iteratively updating the set of outliers. We now briefly introduce Method-M in a simple situation which involves one tumor structure ($s = 1$) and one healthy structure ($s = 2$). We use upper-bound thresholds U_1 and U_2 on the tumor and the healthy structures, respectively, and a smaller upper-bound threshold U_2^{α} such that $U_2^{\alpha} \leq U_2$. It is preferable that each voxel in the healthy structure satisfies the smaller threshold, that is, $z_{2i} \leq U_2^{\alpha}$ for $i = 1, \ldots, |V_2|$. The first LP problem in Method-M is formulated with these ideal constraints. Then the first LP problem is solved, and if these ideal constraints are considered to be too restrictive, the set of outliers $R \subset V_2$ is defined based on the information derived from the first LP problem. Then, the second LP problem will be constructed with the relaxed constraint $z_{2i} \leq U_2$ for $i \in R$ and $z_{2i} \leq U_2^{\alpha}$ for $i \notin R$. In other words, a small set $R \subset V_2$ can be exposed to higher doses than U_2^{α} (note that $U_2 \geq U_2^{\alpha}$). The update of the set R and the construction of the corresponding LP problem will continue until a certain stopping criterion is reached.

Method-M automatically adjusts the set of outliers R, therefore, if we can give an appropriate parameter λ that controls the update of R, we do not need to fix R in advance. On the other hand, this method does not take the fractional parameter α of organs into consideration. The constraints in the LP problems solved involve all the voxels in the structures, and they are often much stronger than the DVCs that are evaluated with only a partial volume of the structure.

2.3 An Approach based on C-VaR type Constraints

Romeijn et al. [16, 15] also utilized LP problems to determine the beamlet intensities, but their approach brought a different perspective. Their method is referred as Method-R in this paper.

A key step of Method-R is to substitute the DVCs with C-VaR type constraints, and this replaces the mixed integer problem (1) into an LP problem. More precisely, an upper DVC

$|\{i \in V_s | z_{si} > U_s^\alpha\}| \leq \alpha |V_s|$ is replaced with a C-VaR type inequality

$$\overline{\zeta}_s^\alpha + \frac{1}{\alpha |V_s|} \sum_{i=1}^{|V_s|} (z_{si} - \overline{\zeta}_s^\alpha)^+ \leq U_s^\alpha, \tag{2}$$

where $\overline{\zeta}_s^\alpha \in \mathbb{R}$ is an additional variable. By introducing the concept of C-VaR into the IMRT optimization, Romeijn et al. [16] proposed the following LP problem:

$$\begin{aligned}
\text{minimize} \quad & \sum_{s=1}^{|S|} \sum_{i=1}^{|V_s|} F_s(z_{si}) && && \text{(3a)}\\
\text{subject to} \quad & \sum_{j=1}^{|B|} D_{sij} x_j = z_{si} && i = 1, \ldots, |V_s|; s = 1, \ldots, |S| && \text{(3b)}\\
& L_s \leq z_{si} \leq U_s && i = 1, \ldots, |V_s|; s = 1, \ldots, |S| && \text{(3c)}\\
& \underline{\zeta}_s^\alpha - \frac{1}{(1-\alpha)|V_s|} \sum_{i=1}^{|V_s|} (\underline{\zeta}_s^\alpha - z_{si})^+ \geq L_s^\alpha && \alpha \in \underline{A}_s; s = 1, \ldots, |S| && \text{(3d)}\\
& \overline{\zeta}_s^\alpha + \frac{1}{\alpha |V_s|} \sum_{i=1}^{|V_s|} (z_{si} - \overline{\zeta}_s^\alpha)^+ \leq U_s^\alpha && \alpha \in \overline{A}_s; s = 1, \ldots, |S| && \text{(3e)}\\
& x_j \geq 0 && j = 1, \ldots, |B| && \text{(3f)}\\
& z_{si} \geq 0 && i = 1, \ldots, |V_s|; s = 1, \ldots, |S| && \text{(3g)}\\
& \overline{\zeta}_s^\alpha : \text{free variable} && \alpha \in \overline{A}_s; s = 1, \ldots, |S| && \text{(3h)}\\
& \underline{\zeta}_s^\alpha : \text{free variable} && \alpha \in \underline{A}_s; s = 1, \ldots, |S| && \text{(3i)}
\end{aligned}$$

Here, the decision variables are the beamlet intensities $x_1, \ldots, x_{|B|}$. To implement the C-VaR type constraints, intermediate variables $\underline{\zeta}_s^\alpha$ and $\overline{\zeta}_s^\alpha$ are employed. As the objective function, a piecewise linear function F_s is employed to minimize an deviation from their desired situation, and this objective function remains (3) as an LP problem.

The validity of C-VaR type constraints in (3) can be provided by the following lemma. Though this claim was partially implied in [15], we provide it in an explicit way.

Lemma 2.1. *Any feasible solution of (3) fulfills all the DVCs.*

Proof: From the constraint (3c), it is clear that the hard DVCs ($L_s \leq z_{si} \leq U_s$) are satisfied.

We now assume that a single upper DVC $|\{i \in V_s | z_{si} > U_s^\alpha\}| \leq \alpha |V_s|$ is violated, and we will derive a contradiction. From this assumption, the number of voxels such that $z_{si} > U_s^\alpha$ is greater than $\alpha |V_s|$. Since $U_s^\alpha \geq \overline{\zeta}_s^\alpha$ from (3e), it holds that $z_{si} > \overline{\zeta}_s^\alpha$ when $z_{si} > U_s^\alpha$. There exists at least one i such that $z_{si} > \overline{\zeta}_s^\alpha$, since $|\{i \in V_s | z_{si} > U_s^\alpha\}| > \alpha |V_s| \geq 0$ from our assumption, hence, we have $(z_{si} - \overline{\zeta}_s^\alpha)^+ = z_{si} - \overline{\zeta}_s^\alpha > U_s^\alpha - \overline{\zeta}_s^\alpha$ for such i. Therefore,

$$\overline{\zeta}_s^\alpha + \frac{1}{\alpha |V_s|} \sum_{i=1}^{|V_s|} (z_{si} - \overline{\zeta}_s^\alpha)^+ > \overline{\zeta}_s^\alpha + \frac{1}{\alpha |V_s|} (\alpha |V_s|) (U_s^\alpha - \overline{\zeta}_s^\alpha) = U_s^\alpha$$

and this contradicts to (3e). Hence, any feasible solution of (3) does not violate the upper DVC. A similar discussion is applicable to the lower DVCs. □

Though this lemma indicates a favorable aspect of Method-R, a negative side is that this approach may fail to find solutions that exist in the gap between the DVCs and the C-VaR type

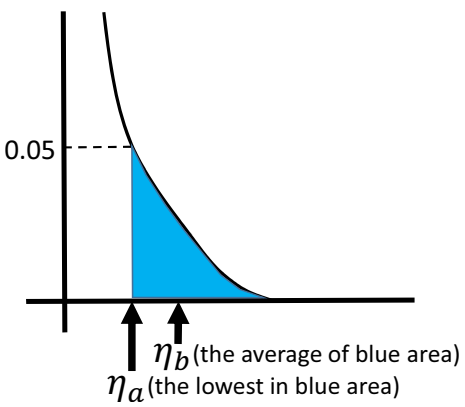

Figure 2: A comparison between DVC and C-VaR type constraint

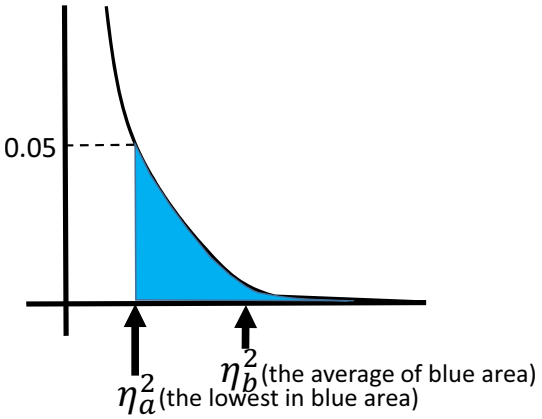

Figure 3: A histogram with a few voxels that receive extremely high doses

constraints (in other words, the converse of Lemma 2.1 does not hold in general). Actually, Method-R searches only a smaller region than the region defined by the original DVCs. Here, we use Figure 2 to compare the DVCs and the C-VaR type constraints in the DVH style. In Figure 2, the blue area corresponds to the top 5% voxels in the structure. When we use η_a to denote the lowest dose among the top 5% voxels, an upper DVC on $\alpha = 0.05$ imposes $\eta_a \leq U_s^{0.05}$. In contrast, the upper C-VaR type constraint (2) requires $\eta_b \leq U_s^{0.05}$, where η_b is the average of the blue area (the average dose of the top 5% voxels). The equivalence between (2) and the constraint $\eta_b \leq U_s^{\alpha}$ is discussed in [16]. Since η_b is larger than η_a, the C-VaR type constraints are tighter than the original DVCs.

Another point we cannot underestimate with respect to the C-VaR type constraints is that the C-VaR type constraints are sensitive to a small number of voxels that receive extreme doses. To demonstrate such a phenomenon, we use Figure 3 which illustrate a similar solution to Figures 2, but it has a few voxels that receive extremely high doses. The lowest doses among the top 5% voxels are almost same in the two figures ($\eta_a \sim \eta_a^2$). On the contrary, their averages of the blue area are significantly different ($\eta_b < \eta_b^2$). Therefore, it is possible that the solution in Figures 2 is feasible ($\eta_b \leq U_s^{0.05}$) while in Figure 3 is infeasible ($\eta_b^2 > U_s^{0.05}$). As shown here, the C-VaR type constraints (3e) strongly depend on the voxels that have the highest doses, hence, such voxels should be handled carefully as outliers.

3 A Successive Linear Programming Approach with C-VaR Type Constraints

In this section, we propose an approach that combines the successive update of outliers and the concept of C-VaR type constraints. In particular, the automatic update of the outliers overcomes the vulnerability of the C-VaR type constraints to the outliers.

In the proposed method, we first solve an LP problem by relaxing the C-VaR type constraints so that this LP problem always has an optimal solution. From the optimal solution of this LP problem, we extract the outliers and delete them from the domain of the C-VaR type constraints. More precisely, in the second LP problem, we replace an upper C-VaR type constraint (3e) for U_s^{α}

with a new constraint

$$\overline{\zeta}_s^{\alpha} + \frac{1}{\alpha|V_s| - |\overline{R}_s^{2,\alpha}|} \sum_{i=1, i \notin \overline{R}_s^{2,\alpha}}^{|V_s|} (z_{si} - \overline{\zeta}_s^{\alpha})^+ \leq U_s^{\alpha} + \overline{P}_s^{\alpha} t. \tag{4}$$

Here, the $\overline{R}_s^{2,\alpha}$ is the set of outliers detected by the first LP problem. Compared to (3e), the summation in the second term of (4) skips the outliers $\overline{R}_s^{2,\alpha}$, and the denominator is reduced from $\alpha|V_s|$ to $\alpha|V_s| - |\overline{R}_s^{2,\alpha}|$. The last term in the right hand side by a positive constant $\overline{P}_s^{\alpha}$ and a new nonnegative variable $t \in \mathbb{R}$ is added to guarantee the existence of an optimal solution in the second LP problem. After solving the second LP problem with the new constraint (4), we select the new outliers $\overline{R}_s^{3,\alpha}$ for the third LP problem as a set of the voxels that receive extreme doses based on a criterion $\overline{R}_s^{3,\alpha} = \{i \in V_s : z_{si}^{(2)} > U_s^{\alpha} + \overline{P}_s^{\alpha} t^{(2)}\}$, where $z_{si}^{(2)}$ and $t^{(2)}$ are parts of the optimal solution of the second LP problem. Then we solve the third LP problem and update the outliers for $\overline{R}_s^{4,\alpha}$. We iterate the construction of the LP problems and the updates of outliers, until we obtain a feasible solution that satisfies the original DVCs. The proposed method has favorable properties, which will be considered later in Theorem 3.2.

Here, we are focused on an effect of excluding outliers from the C-VaR type constraints. Figure 4 compares an original DVC $|\{i \in V_s | z_{si} > U_s^{\alpha}\}| \leq \alpha|V_s|$, its corresponding C-VaR type constraint (3e) and the constraint of the proposed method (4) in the style of DVH. In this figure, the union of the blue and red areas is the top 5% voxels in the structure s, and the red area corresponds to the outliers R that receive extremely high doses. The original DVC imposes $\eta_a \leq U_s^{0.05}$ and the C-VaR type constraint (3e) requires $\eta_b \leq U_s^{0.05}$.

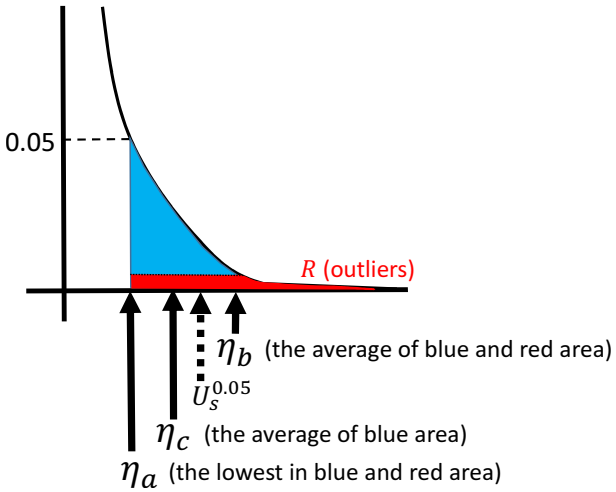

Figure 4: An effect of the removal of outliers

The removal of outliers R (the red area) changes the average from η_b to η_c, where η_c is the average of the blue area. The gap of Method-R from the original DVCs is $\eta_b - \eta_a$ and that of the proposed method is $\eta_c - \eta_a$. In particular, if the number of outliers is very few ($|R| << |V_s|$), we can expect $\eta_c \sim \eta_a$. Hence, the proposed method is closer to the original DVCs than Method-R. In addition, if $U_s^{0.05}$ lies in the interval $\eta_c < U_s^{0.05} < \eta_b$, this solution is out of the C-VaR type constraint, but the proposed method detects that this solution satisfies the DVCs.

Consequently, the proposed method searches a feasible solution in a wider region than Method-R, and its computation cost is much low compared to the original DVCs (the computational

complexity of the original DVCs is NP-hard [17]). We also remark that the update of outliers is carried out automatically from the solution of LP problems.

The framework of the proposed method is outlined in Algorithm 3.1. In the kth LP problem of Step 2, we use $\overline{R}_s^{k,\alpha}$ and $\underline{R}_s^{k,\alpha}$ to denote the sets of outliers with respect to the fractions $\alpha \in \overline{A}_s$ and $\alpha \in \underline{A}_s$, respectively. In addition, the objective function t is used to minimize the deviation from the DVCs.

Algorithm 3.1. *A successive update of outliers with C-VaR type constraints for FMO problems*

1. Set the iteration counter $k = 1$ and the initial sets of outliers $\overline{R}_s^{1,\alpha} = \emptyset$ for $\alpha \in \overline{A}_s, s \in S$ and $\underline{R}_s^{1,\alpha} = \emptyset$ for $\alpha \in \underline{A}_s, s \in S$. Choose positive constants $\overline{P}_s$ and $\underline{P}_s$ for $s \in S$, $\overline{P}_s^\alpha$ for $\alpha \in \overline{A}_s, s \in S$, and $\underline{P}_s^\alpha$ for $\alpha \in \underline{A}_s, s \in S$.

2. Solve the following kth LP. Let $t^{(k)}$ be the optimal value of this LP problem, and $x_j^{(k)}$ and $z_{si}^{(k)}$ be the obtained solution.

$$\begin{aligned}
\min \quad & t && && \text{(5a)}\\
\text{s.t.} \quad & \sum_{j=1}^{|B|} D_{sij} x_j = z_{si} && i \in V_s; s \in S && \text{(5b)}\\
& L_s - \underline{P}_s t \le z_{si} \le U_s + \overline{P}_s t && i \in V_s; s \in S && \text{(5c)}\\
& \underline{\zeta}_s^\alpha - \frac{1}{(1-\alpha)|V_s| - |\underline{R}_s^{k,\alpha}|} \sum_{\substack{i=1 \\ i \notin \underline{R}_s^{k,\alpha}}}^{|V_s|} (\underline{\zeta}_s^\alpha - z_{si})^+ \ge L_s^\alpha - \underline{P}_s^\alpha t && \alpha \in \underline{A}_s; s \in S && \text{(5d)}\\
& \overline{\zeta}_s^\alpha + \frac{1}{\alpha|V_s| - |\overline{R}_s^{k,\alpha}|} \sum_{i=1, i \notin \overline{R}_s^{k,\alpha}}^{|V_s|} (z_{si} - \overline{\zeta}_s^\alpha)^+ \le U_s^\alpha + \overline{P}_s^\alpha t && \alpha \in \overline{A}_s; s \in S && \text{(5e)}\\
& x_j \ge 0 && j \in B && \text{(5f)}\\
& z_{si} \ge 0 && i \in V_s; s \in S && \text{(5g)}\\
& \overline{\zeta}_s^\alpha : \text{free variable} && \alpha \in \overline{A}_s; s \in S && \text{(5h)}\\
& \underline{\zeta}_s^\alpha : \text{free variable} && \alpha \in \underline{A}_s; s \in S && \text{(5i)}\\
& t : \text{free variable} && && \text{(5j)}
\end{aligned}$$

3. If $t^{(k)} \le 0$, output $\boldsymbol{x}^{(k)}$ as the solution and stop.

4. Update the sets of outliers by the rules

$$\overline{R}_s^{k+1,\alpha} := \left\{ i \in V_s : z_{si}^{(k)} > U_s^\alpha + \overline{P}_s^\alpha t^{(k)} \right\}, \quad \underline{R}_s^{k+1,\alpha} := \left\{ i \in V_s : z_{si}^{(k)} < L_s^\alpha - \underline{P}_s^\alpha t^{(k)} \right\}.$$

   Increment k and return to Step 2.

The proposed method enjoys the following suitable properties.

Theorem 3.2. *We assume that the feasible region $\mathcal{F}$ of the FMO problem (1) is not empty. Then, for LP problems solved in Algorithm 3.1, it holds that*

(a) For any $k \ge 1$, the kth LP problem (5) has an optimal solution.

(b) If $t^{(k)} \leq 0$, the output solution $\boldsymbol{x}^{(k)}$ satisfies all the DVCs (that is, $\boldsymbol{x}^{(k)} \in \mathcal{F}$).

(c) The sequence $\{t^{(k)}\}$ is monotonically non-increasing.

Part (a) indicates that the solution $\boldsymbol{x}^{(k)}$ is well-defined through Algorithm 3.1. Part (b) provides a validity for the stopping criterion $t^{(k)} \leq 0$ in Step 3. Finally, we can infer from Part (c) that the sequence $\{\boldsymbol{x}^{(k)}\}$ is inclined to approach to the set that satisfy all the DVCs.

We remark that the solution obtained from Method-R corresponds to $\boldsymbol{x}^{(1)}$ of Algorithm 3.1 with the parameters $\overline{P}_s = \underline{P}_s = \overline{P}_s^{\alpha} = \underline{P}_s^{\alpha} = 0$ for all s and α. From Part(c), therefore, the proposed method is more flexible than Method-R.

Proof: For Part(a), we first examine the case $k = 1$ and discuss $k \geq 2$ by induction. At the beginning of $k = 1$, $\underline{R}_s^{1,\alpha}$ and $\overline{R}_s^{1,\alpha}$ are empty sets. Then, the denominators in (5d) and (5e) are not zero, as $|V_s| > 0$ without loss of generality and $0 < \alpha < 1$. The first LP problem ($k = 1$) is well-defined, and we can give a feasible solution explicitly by $x_j = 0$ ($j = 1, \ldots, |B|$), $z_{si} = 0$ ($i = 1, \ldots, |V_s|, s = 1, \ldots, |S|$), $\overline{\zeta}_s^{\alpha} = 0$ ($\alpha \in \overline{A}_s, s = 1, \ldots, |S|$), $\underline{\zeta}_s^{\alpha} = 0$ ($\alpha \in \underline{A}_s, s = 1, \ldots, |S|$) and $t = \min_{s=1,\ldots,|S|} \left\{ L_s/\underline{P}_s, \min_{\alpha \in \underline{A}_s^{\alpha}} \{L_s^{\alpha}/\underline{P}_s^{\alpha}, \} \right\}$. We also know that

$$\begin{aligned} & \overline{\zeta}_s^{\alpha} + \frac{1}{\alpha|V_s| - |\overline{R}_s^{k,\alpha}|} \sum_{i=1, i \notin \overline{R}_s^{k,\alpha}}^{|V_s|} (z_{si} - \overline{\zeta}_s^{\alpha})^+ = \overline{\zeta}_s^{\alpha} + \frac{1}{\alpha|V_s|} \sum_{i=1}^{|V_s|} (z_{si} - \overline{\zeta}_s^{\alpha})^+ \\ \geq \; & \overline{\zeta}_s^{\alpha} + \frac{1}{|V_s|} \sum_{i=1}^{|V_s|} (z_{si} - \overline{\zeta}_s^{\alpha})^+ = \frac{1}{|V_s|} \sum_{i=1}^{|V_s|} \left\{ \overline{\zeta}_s^{\alpha} + (z_{si} - \overline{\zeta}_s^{\alpha})^+ \right\} \geq 0. \end{aligned}$$

The last inequality holds from an inequality $p + (q-p)^+ \geq 0$ for any $p \in \mathbb{R}$ and $q \geq 0$. From (5c) and (5e), the objective function t has a lower bound $t \geq \max \left\{ \max_{s=1,\ldots,S} \left\{ -U_s/\overline{P}_s \right\}, \max_{\alpha \in \overline{A}_s^{\alpha}} \left\{ -U_s^{\alpha}/\overline{P}_s^{\alpha} \right\} \right\}$. From the duality theorem of linear programming [4, etc], the first LP problem has an optimal value $t^{(1)}$.

Next, we assume that the kth LP has its optimal value $t^{(k)}$ and optimal solution $x_i^{(k)}$ and $z_{si}^{(k)}$, and we examine the $(k+1)$th LP. If the number of voxels in V_s such that $z_{si}^{(k)} > U_s^{\alpha} + \overline{P}_s^{\alpha} t^{(k)}$ and $i \notin \overline{R}_s^{k,\alpha}$ were no less than $\alpha|V_s| - \overline{R}_s^{k,\alpha}$, we would have

$$\begin{aligned} \overline{\zeta}_s^{\alpha} + \frac{1}{\alpha|V_s| - |\overline{R}_s^{k,\alpha}|} \sum_{i=1, i \notin \overline{R}_s^{k,\alpha}}^{|V_s|} (z_{si}^{(k)} - \overline{\zeta}_s^{\alpha})^+ \; &> \; \overline{\zeta}_s^{\alpha} + \frac{1}{\alpha|V_s| - |\overline{R}_s^{k,\alpha}|} (\alpha|V_s| - |\overline{R}_s^{k,\alpha}|)(U_s^{\alpha} + \overline{P}_s^{\alpha} t^{(k)} - \overline{\zeta}_s^{\alpha}) \\ &= \; U_s^{\alpha} + \overline{P}_s^{\alpha} t^{(k)}, \end{aligned}$$

but this contradicts (5e). Hence, the increase in the number of outliers is bounded by $\alpha|V_s| - |\overline{R}_s^{k,\alpha}|$, and this leads to

$$|\overline{R}_s^{k+1,\alpha}| < (\alpha|V_s| - |\overline{R}_s^{k,\alpha}|) + |\overline{R}_s^{k,\alpha}| = \alpha|V_s|. \tag{6}$$

For the lower DVCs, we also obtain $|\underline{R}_s^{k+1,\alpha}| < (1-\alpha)|V_s|$. Therefore, the denominators in (5e) and (5d) are not zero again, and we can use the same discussion as the first LP problem above to derive that the $(k+1)$th LP has an optimal value $t^{(k+1)}$. By induction, for any $k \geq 1$, the kth LP has its optimal value $t^{(k)}$.

For Part (b), from the definition of $\overline{R}_s^{k+1,\alpha} = \left\{ i \in V_s : z_{si}^{(k)} > U_s^{\alpha} + \overline{P}_s^{\alpha} t^{(k)} \right\}$, the non-positivity of $t^{(k)}$ indicates that $\{i \in V_s : z_{si}^{(k)} > U_s^{\alpha}\} \subset \overline{R}_s^{k+1,\alpha}$. Using the upper bound on the size of $\overline{R}_s^{k+1,\alpha}$ obtained in (6), we have $|\{i \in V_s : z_{si}^{(k)} > U_s^{\alpha}\}| \leq |\overline{R}_s^{k+1,\alpha}| \leq \alpha|V_s|$ and this means the solution

of kth LP problem satisfies the corresponding upper DVCs. We can also demonstrate that the solution with non-positive $t^{(k)}$ satisfies the lower DVCs in a similar way.

Finally, in order to verify the inequality $t^{(k+1)} \leq t^{(k)}$ for Part (c), we give a feasible solution of the $(k+1)$th LP problem such that $t = t^{(k)}$. We set $t = t^{(k)}$, $x_j = x_j^{(k)}$, $z_{si} = z_{si}^{(k)}$, $\underline{\zeta}_s^{\alpha} = L_s^{\alpha} - \underline{P}_s^{\alpha} t^{(k)}$ and $\overline{\zeta}_s^{\alpha} = U_s^{\alpha} + \overline{P}_s^{\alpha} t^{(k)}$. Since these values are derived from the kth LP problem, it is easy to check that these values satisfy the constraints of (5) except (5e) and (5d). In (5e), the summation $\sum_{i=1, i \notin \overline{R}_s^{k+1,\alpha}}^{|V_s|} (z_{si} - \overline{\zeta}_s^{\alpha})^+$ is zero due to $\overline{R}_s^{k+1,\alpha} = \left\{ i \in V_s : z_{si}^{(k)} > U_s^{\alpha} + \overline{P}_s^{\alpha} t^{(k)} \right\}$ and $\overline{\zeta}_s^{\alpha} = U_s^{\alpha} + \overline{P}_s^{\alpha} t^{(k)}$. Therefore, the left-hand side of (5e) reduces to $U_s^{\alpha} + \overline{P}_s^{\alpha} t^{(k)}$ and this is same as the right-hand side. Again, we apply a similar step to (5d). □

4 Numerical Experiment

For a numerical experiment, we used a dataset of the American Association of Physicists in Medicine (AAPM) Task Group (TG) 119 report [7]. The dataset includes four mock test cases; a C-shape case, a mock prostate case, a mock head/neck case and a multi target case. For these four cases, Table 1 shows the number of beamlets, the organ names, the number of voxels in the organs and the DVCs.

We compare the proposed method with Method-M to show the performance of the proposed method. We did not use Method-R in the numerical comparison, since we found from preliminary experiments that the LP problems in the Method-R were infeasible for all of the four test cases in AAPM TG119.

The dataset of AAPM TG119 is provided as 3D image format called DICOM. Using CERR 4.0 Beta 2 [5] and MATLAB 2017a, we transformed the DICOM files into the LP problems (5). We ran CERR with its default settings, then we called CPLEX 12.7.1 to solve the generated LP problems. Finally, we utilized CERR again to visualize the solutions and checked whether the obtained solutions satisfied the DVCs. We also utilized CERR to prepare a manageable dataset from the TG119 dataset. The number of voxels in PTV of the mock head/neck case was more than 50,000 and this was too large to solve (5) on 16 GB memory space of our computing environment. For only this case, therefore, we chose 10,000 voxels randomly from the 50,000 voxels. We examined a number of this random selection and we observed this operation did not affect the numerical results seriously. The computing environment was a server powered by two Opteron 4386 (3.1 GHz, 8 cores) processors with a RAM of 16 GB running on a Debian Linux operating system.

A desirable stopping criterion of the proposed method is $t^{(k)} \leq 0$, since Theorem 3.2 indicated that the output solution $\boldsymbol{x}^{(k)}$ satisfies all the DVCs when $t^{(k)} \leq 0$. Due to the intrinsic difficulty arising from combinatorial aspects of the DVCs, the number of iterations to attain $t^{(k)} \leq 0$ would be prohibitive. As practical stopping criteria, we stopped the proposed method when the iteration count k reached 10, or when the objective value did not improve ($|t^{(k)} - t^{(k-1)}| < 10^{-4}$). In the execution of the proposed method, we assigned 1 to the positive constants $\underline{P}_s, \overline{P}_s, \underline{P}_s^{\alpha}$, and $\overline{P}_s^{\alpha}$.

For Method-M, we set the parameter $\lambda = 10^{-6}$, which controls the update of the set of outliers R. In addition, we stopped Method-M when the set R became infeasible for a DVC; more precisely, when $|R|$ exceeded $\alpha|V_s|$. When the infeasibility was detected at the kth iteration, the solution of Method-M was extracted from the solution of the LP problem in the $(k-1)$th iteration.

4.1 Results

Table 2 reports the satisfiability of the obtained solutions for given DVCs, and Figures 5, 6, 7, and 8 provide the DVH figures. In these figures, the solid lines and the broken lines indicate the

Table 1: A summary of the dataset for numerical comparison

C-shape (the number of beamlets is 414)				
organ/tumor	the number of voxels	DVCs		
Outer Target	17522	$L^{0.95}_{\text{Outer Target}}$	=	50
		$U^{0.1}_{\text{Outer Target}}$	=	55
Core	3087	$U^{0.1}_{\text{Core}}$	=	25
Mock Head/Neck (the number of beamlets is 619)				
organ/tumor	the number of voxels	DVCs		
PTV	10000	$L^{0.99}_{\text{PTV}}$	=	46.5
		$L^{0.9}_{\text{PTV}}$	=	50.0
		$U^{0.2}_{\text{PTV}}$	=	55
Cord	1333	U_{Cord}	=	40
Lt Parotid	525	$U^{0.5}_{\text{Lt Parotid}}$	=	20
Rt Parotid	740	$U^{0.5}_{\text{Rt Parotid}}$	=	20
Mock Prostate (the number of beamlets is 241)				
organ/tumor	the number voxels	DVCs		
Prostate PTV	8591	$L^{0.95}_{\text{Prostate PTV}}$	=	75.6
		$U^{0.05}_{\text{Prostate PTV}}$	=	83
Urinary Bladder	5207	$U^{0.30}_{\text{Urinary Bladder}}$	=	70
		$U^{0.10}_{\text{Urinary Bladder}}$	=	75
Rectum	1830	$U^{0.30}_{\text{Rectum}}$	=	70
		$U^{0.10}_{\text{Rectum}}$	=	75
Multi Target (the number of beamlets is 601)				
organ/tumor	the number of voxels	DVCs		
Center	5143	$L^{0.99}_{\text{Center}}$	=	50
		$U^{0.1}_{\text{Center}}$	=	53
Superior	5549	$L^{0.99}_{\text{Superior}}$	=	25
		$U^{0.1}_{\text{Superior}}$	=	35
Inferior	5529	$L^{0.99}_{\text{Inferior}}$	=	12.5
		$U^{0.1}_{\text{Inferior}}$	=	25

results of the proposed method and Method-M, respectively, and different colors are utilized to clarify the organs.

In Table 2, the column "proposed" indicates the evaluation of the proposed method in the viewpoint of DVCs. For example, the value of 50.5 in the row $L^{0.95}_{\text{Outer Target}}$ indicates that 95% of Outer Target receives at least 50.5 Gy. Therefore, this solution satisfies $L^{0.95}_{\text{Outer Target}} = 50.0$ and this satisfiability is shown by "Pass." The failure of the solutions is indicated by "Fail" in the table. In the same way, the column "Method-M" shows the result of Method-M. The table also reports the numbers of LP problems solved in each test case. The number of parenthesis in the "proposed" column shows the number of LP problems to acquire a feasible solution. In the C-shape case, for example, the proposed method obtained a feasible solution by the third LP problem ($t^{(3)} \leq 0$), and stopped the computation by the criterion $t^{(4)} = t^{(3)}$. (In the Multi Target case, we used $(-)$ to indicate that we failed to obtain a non-positive optimal value before we stopped the computation by $t^{(7)} = t^{(6)}$.) The last two rows in each test case report the computation time for LP problems and the total running time.

From the result of Table 2, we observe in the C-Shape case that the solution of the proposed method satisfied all DVCs, but Method-M failed in the DVC $L^{0.95}_{\text{Outer Target}} = 50.0$. We also see that the green dashed line passes the point $(50, 0.5)$ in Figure 5, therefore, a half of the voxels of Outer Target in Method-M receives 50 Gy or less. The proposed method fits the lower DVCs more appropriately than Method-M. We can further obtain similar observations on the Head/Neck and Prostate cases.

For the Multi Target case, however, Table 2 shows that both the proposed method and Method-M failed to satisfy all the DVCs simultaneously. In particular, the DVC ($L^{0.99}_{\text{Center}} = 50$) seems too stringent. In Section 5, we will investigate a relaxation of this stringent DVC and discuss its effect. Except this DVC $L^{0.99}_{\text{Center}} = 50$, the proposed method and Method-M satisfied the other DVCs.

Consequently, the proposed method output solutions that match the DVCs more adequately than Method-M in three cases and a competitive solution for the Multi Target case.

Next, we move our focus to the computation time. Most of the computation time in both the proposed method and Method-M was the execution of CPLEX to solve the generated LP problems. CPLEX accounted for at least 95% of the total running time, while the computation time to generate LP problems using outliers was short. Each iteration of the proposed method was longer than that of Method-M, but the number of iterations in the proposed method was considerably smaller than Method-M, particularly in Mock Head/Neck and Prostate cases. Therefore, the proposed method is preferable to Method-M from the viewpoint of computation cost.

5 Discussions

In this paper, we propose a new iterative algorithm for the FMO problems. Here, we discuss several aspects of the proposed method.

Parameters for Method-M

There would be a possibility that a judicious selection on the parameters for Method-M might improve the quality of the solution or the running time. In the numerical experiments, we examined Method-M changing the parameters and we reported the best results of Method-M from the changed parameters, so further improvements based on only the parameter selection are not so promising.

For Method-M, a reduction of the computation time is also a difficult task. For example, to solve one LP problem in the C-shape case, the proposed method consumed about twice computation time of Method-M. However, the proposed method acquired a feasible solution in the three iterations.

Table 2: Numerical results for the four test cases

C-Shape			
organ/tumor	DVCs	proposed	Method-M
Outer Target	$L^{0.95}_{\text{Outer Target}} = 50.0$	50.5 (Pass)	45.7 (Fail)
	$U^{0.10}_{\text{Outer Target}} = 55.0$	54.4 (Pass)	53.9 (Pass)
Core	$U^{0.10}_{\text{Core}} = 25.0$	24.3 (Pass)	25.0 (Pass)
the number of iterations		4 (3)	13
time for LP problems (second)		94.489	223.237
total time (second)		100.870	230.999
Mock Head/Neck			
organ/tumor	DVCs	proposed	Method-M
PTV	$L^{0.99}_{\text{PTV}} = 46.5$	48.5 (Pass)	40.7 (Fail)
	$L^{0.90}_{\text{PTV}} = 50.0$	51.2 (Pass)	42.4 (Fail)
	$U^{0.20}_{\text{PTV}} = 55.0$	53.8 (Pass)	52.3 (Pass)
Core	$U_{\text{Core}} = 40.0$	39.0 (Pass)	40.0 (Pass)
Lt Parotid	$U^{0.50}_{\text{Lt Parotid}} = 20.0$	15.8 (Pass)	20.0 (Pass)
Rt Parotid	$U^{0.50}_{\text{Rt Parotid}} = 20.0$	14.8 (Pass)	17.4 (Pass)
the number of iterations		3 (2)	27
time for LP problems (second)		76.124	468.667
total time (second)		78.078	479.753
Prostate			
organ/tumor	DVCs	proposed	Method-M
Prostate PTV	$L^{0.95}_{\text{Prostate PTV}} = 75.6$	76.7 (Pass)	73.7 (Fail)
	$U^{0.05}_{\text{Prostate PTV}} = 83.0$	82.2 (Pass)	82.0 (Pass)
Urinary Bladder	$U^{0.30}_{\text{Urinary Bladder}} = 70.0$	49.6 (Pass)	53.3 (Pass)
	$U^{0.10}_{\text{Urinary Bladder}} = 75.0$	72.2 (Pass)	65.8 (Pass)
Rectum	$U^{0.30}_{\text{Rectum}} = 70.0$	67.0 (Pass)	70.0 (Pass)
	$U^{0.10}_{\text{Rectum}} = 75.0$	73.9 (Pass)	74.8 (Pass)
the number of iterations		3 (2)	22
time for LP problems (second)		106.419	699.439
total time (second)		108.078	709.672
Multi Target			
organ/tumor	DVCs	proposed	Method-M
Center	$L^{0.99}_{\text{Center}} = 50.0$	46.1 (Fail)	43.6 (Fail)
	$U^{0.10}_{\text{Center}} = 53.0$	52.6 (Pass)	52.5 (Pass)
Superior	$L^{0.99}_{\text{Superior}} = 25.0$	25.7 (Pass)	33.5 (Pass)
	$U^{0.10}_{\text{Superior}} = 35.0$	34.5 (Pass)	35.0 (Pass)
Inferior	$L^{0.99}_{\text{Inferior}} = 12.5$	12.8 (Pass)	21.9 (Pass)
	$U^{0.10}_{\text{Inferior}} = 25.0$	24.8 (Pass)	25.0 (Pass)
the number of iterations		7 (-)	15
time for LP problems (second)		215.875	316.304
total time (second)		219.859	323.660

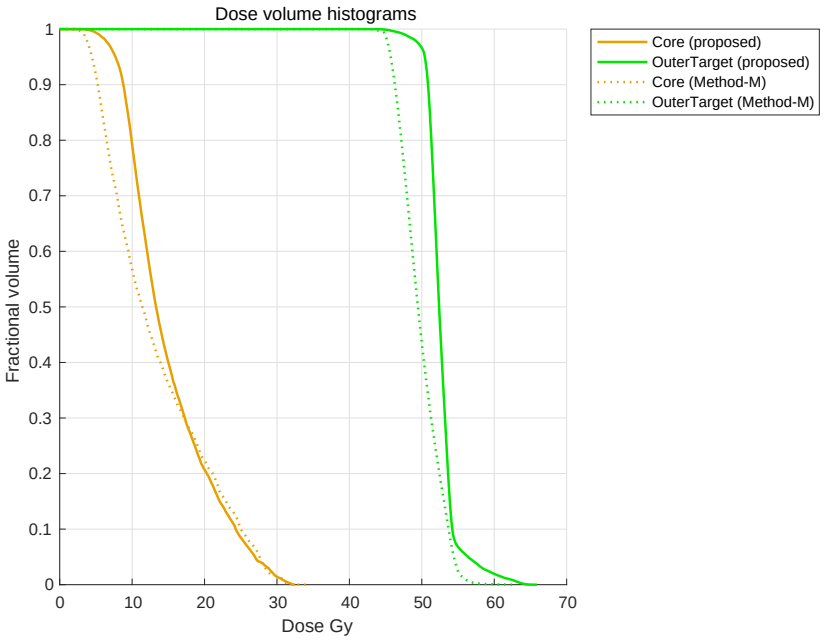

Figure 5: DVH of C-Shape case

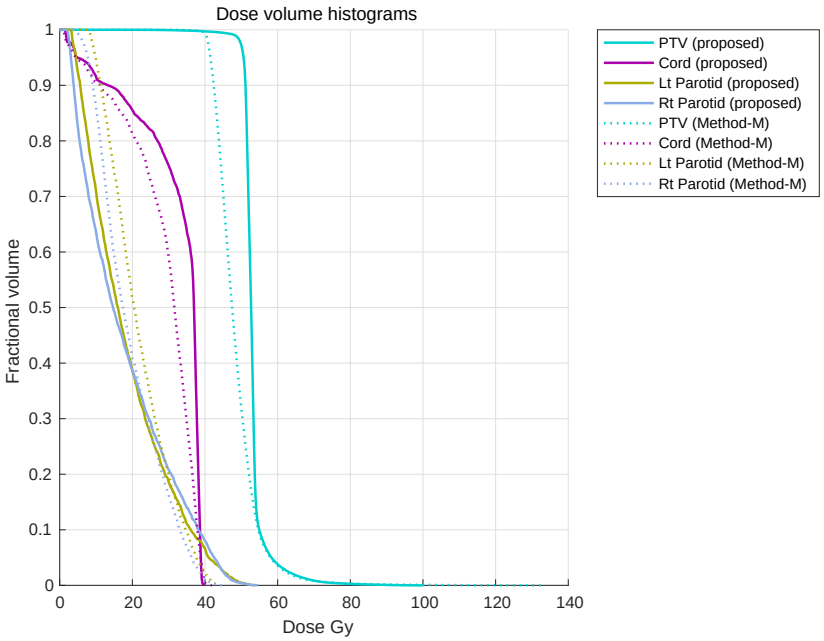

Figure 6: DVH of Head/Neck case

To compete with the proposed method, therefore, Method-M should complete its algorithm within about six iterations, but Method-M actually required 13 iterations.

We remark that the number of intermediate variables in the LP problems of the proposed method is dependent on the number of DVCs, while that of Method-M is independent. The test cases we used in the numerical tests have a few DVC, therefore, Method-M may perform well in a

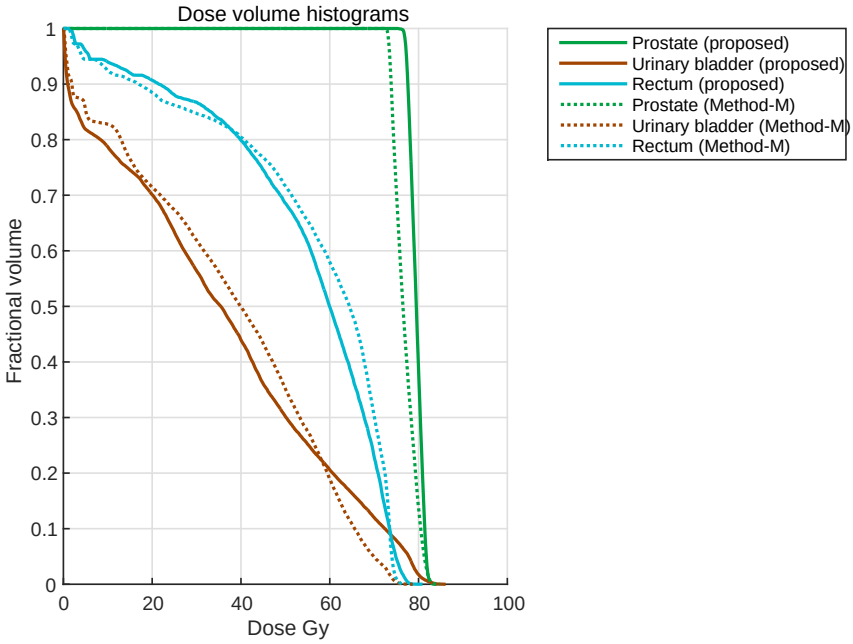

Figure 7: DVH of Prostate case

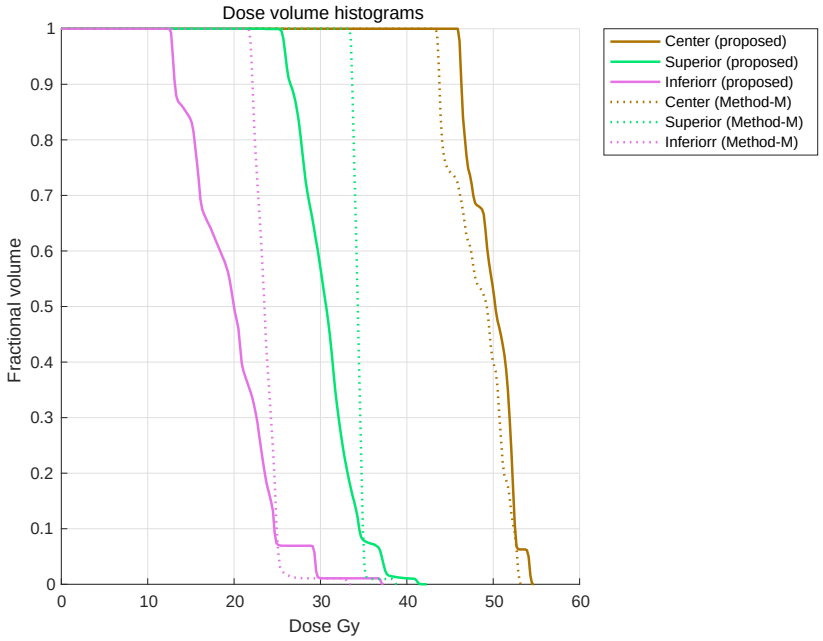

Figure 8: DVH of Multi Target case

test case that includes a large number of DVCs.

The result on Multi Target

In the Multi Target case, both the proposed method and Method-M failed to satisfy the DVC $L^{0.99}_{\text{Center}} = 50$. Here, we discuss an effect brought by a relaxation on this stringent DVC.

First, the objective value in the last LP problem of the proposed method was $t^{(7)} = 4.8$, and even when we continued the computation with additional 20 iterations, we could not improve this objective value. For this $t^{(7)}$, the right hand side in the inequality (5c) is $L^{0.99}_{\text{Center}} - \underline{P}^{0.99}_{\text{Center}} t^{(7)} = 50 - 1 \cdot 4.8 = 45.2$. Using this value, we examined a replacement of the stringent DVC $L^{0.99}_{\text{Center}} = 50$ by an weaker DVC $\widehat{L}^{0.99}_{\text{Center}} = 45.2$. Table 3 summarizes the results on this weaker DVC in the same style as Table 2.

Table 3: Numerical results for Multi Target with an weaker DVC

Multi Target			
organ/tumor	DVCs	proposed	Method-M
Center	$\widehat{L}^{0.99}_{\text{Center}} = 45.2$	46.1 (Pass)	43.6 (Fail)
	$U^{0.10}_{\text{Center}} = 53.0$	52.6 (Pass)	52.5 (Pass)
Superior	$L^{0.99}_{\text{Superior}} = 25.0$	26.7 (Pass)	33.5 (Pass)
	$U^{0.10}_{\text{Superior}} = 35.0$	34.4 (Pass)	35.0 (Pass)
Inferior	$L^{0.99}_{\text{Inferior}} = 12.5$	12.8 (Pass)	21.9 (Pass)
	$U^{0.10}_{\text{Inferior}} = 25.0$	24.8 (Pass)	25.0 (Pass)
the number of iterations		4 (3)	14
time for LP problems (second)		124.530	317.338
total time (second)		126.549	324.636

The result of Method-M in Table 3 remained essentially same as Table 2, and it still could not satisfy $\widehat{L}^{0.99}_{\text{Center}} = 45.2$, hence we cannot see the effect of the relaxation. Though the result of Method-R does not appear in Table 2, it also failed in this weaker DVC. On the contrary, the proposed method managed to find a solution that satisfied all the DVCs including $\widehat{L}^{0.99}_{\text{Center}} = 45.2$. Consequently, the necessary modification on the stringent DVC was small in the proposed method compared to Method-M and Method-R. From this result, we infer that the objective value $t^{(k)}$ in the proposed method can be employed to evaluate stringency of the DVCs.

An extension of our approach to precise volumes

In this paper, we assumed that an organ was divided into voxels of the same rectangular shape, thus all the voxels had the same volume. However, voxels at the boundary of a structure may partially contain the exterior of the structure. Therefore, there may be a difference between the total volume of voxels in the structure and the precise volume, and our approach would output a solution with minor deviations.

Our approach can be extended to handle the precise volume of each voxel by the procedure below. For the ith voxel of the structure s, c_{si} is used to denote the volume of a part of s that is covered by the ith voxel, in other words, c_{si} is the volume of the intersection of s and the ith voxel. Then, a constant $C_s := \sum_{i=1}^{|V_s|} c_{si}$ denotes the precise volume of s. We also define $\overline{C}^{k,\alpha}_s := \sum_{i \in \overline{R}^{k,\alpha}_s} c_{si}$ and $\underline{C}^{k,\alpha}_s := \sum_{i \in \underline{R}^{k,\alpha}_s} c_{si}$ for upper and lower DVCs, respectively.

We will replace the kth LP problem in Algorithm 3.1 with the following LP problem:

$$\text{minimize} \quad t \tag{7a}$$

$$\text{subject to} \quad \sum_{j=1}^{|B|} D_{sij} x_j = z_{si} \qquad i \in V_s; s \in S \tag{7b}$$

$$L_s - \underline{P}_s t \le z_{si} \le U_s + \overline{P}_s t \qquad i \in V_s; s \in S \tag{7c}$$

$$\underline{\zeta}_s^\alpha - \frac{1}{(1-\alpha)C_s - \underline{C}_{ks}^\alpha} \sum_{i \notin \underline{R}_s^{k,\alpha}} c_{si}(\underline{\zeta}_s^\alpha - z_{si})^+ \ge L_s^\alpha - \underline{P}_s^\alpha t \quad \alpha \in \underline{A}_s; s \in S \tag{7d}$$

$$\overline{\zeta}_s^\alpha + \frac{1}{\alpha C_s - \overline{C}_s^{k,\alpha}} \sum_{i \notin \overline{R}_s^{k,\alpha}} c_{si}(z_{si} - \overline{\zeta}_s^\alpha)^+ \le U_s^\alpha + \overline{P}_s^\alpha t \qquad \alpha \in \overline{A}_s; s \in S \tag{7e}$$

$$x_j \ge 0 \qquad j \in B \tag{7f}$$

$$z_{si} \ge 0 \qquad i \in V_s; s \in S \tag{7g}$$

$$\underline{\zeta}_s^\alpha : \text{free variables} \qquad \alpha \in \underline{A}_s; s \in S \tag{7h}$$

$$\overline{\zeta}_s^\alpha : \text{free variables} \qquad \alpha \in \overline{A}_s; s \in S \tag{7i}$$

$$t : \text{free variables} \tag{7j}$$

A main difference between the original proposed method and this extended method lies in (5d) and (7d). In the original proposed method, we use the number of voxels to represent a fractional volume of the structure. However, in the extended method, we utilize their precise volumes, therefore, we include c_{si} in the summation of (7d). This LP problem satisfies the same property as Theorem 3.2. In particular, we can find a solution that satisfies all the DVCs when the optimal value $t^{(k)}$ of the kth LP problem is non-positive. Therefore, we can naturally extend the proposed method to handle the precise volumes.

6 Conclusion and Future Directions

In this paper, we proposed a novel method for the FMO problems by combining the C-VaR type constraints and the automatic update of the outliers. The proposed method has favorable mathematical properties as discussed in Theorem 3.2. In particular, when the optimal value of the LP problems is non-positive, its optimal solution satisfies all the DVCs. From the numerical experiments, we verified that the proposed method was effective for the mock cases. The proposed method found feasible solutions for the test cases whose feasibilities were not detected in Method-R. Furthermore, our approach obtained these feasible solutions within a shorter computation time than Method-M.

Further studies should include improvement in the computation time. The size of LP problems in the proposed method is highly dependent on the number of DVCs, therefore, the computation time to solve the LP problems grows rapidly, especially when the number of DVCs increases. As a result, the size of solvable FMO problems are limited. We should reduce the number of variables involved in the LP problems in advance by detecting redundant variables or inactive constraints.

Another aspect is that the proposed method could not satisfy only one DVC in the Multi Target case, therefore, we relaxed only this DVC and we managed to find a feasible solution that satisfied all the DVCs. If the proposed method could not satisfy multiple DVCs, there is room for further discussions on how to adjust them simultaneously. For example, we may exploit an multi-criteria optimization discussed in [6].

Acknowledgments

The authors would like to thank anonymous referees for valuable suggestions to improve the quality of this paper. In particular, the discussions of the relaxation of the stringent DVCs in Section 5 originated from the referees' comments.

References

[1] D. M. Aleman, D. Glaser, H. E. Romeijn, and J. F. Dempsey. Interior point algorithms: guaranteed optimality for fluence map optimization in IMRT. *Physics in Medicine and Biology*, 55(18):5467, 2010.

[2] G. Bednarz, D. Michalski, C. Houser, M. S. Huq, Y. Xiao, P. R. Anne, and J. M. Galvin. The use of mixed-integer programming for inverse treatment planning with pre-defined field segments. *Physics in Medicine and Biology*, 47(13):2235, 2002.

[3] T. C. Chan, H. Mahmoudzadeh, and T. G. Purdie. A robust-cvar optimization approach with application to breast cancer therapy. *European Journal of Operational Research*, 238(3):876–885, 2014.

[4] V. Chvatal. *Linear programming*. Macmillan, 1983.

[5] J. O. Deasy, A. I. Blanco, and V. H. Clark. CERR: a computational environment for radiotherapy research. *Medical Physics*, 30(5):979–985, 2003.

[6] L. Engberg, A. Forsgren, K. Eriksson, and B. Hardemark. Explicit optimization of plan quality measures in intensity-modulated radiation therapy treatment planning. *Medical Physics*, 2017.

[7] G. A. Ezzell, J. W. Burmeister, N. Dogan, T. J. LoSasso, J. G. Mechalakos, D. Mihailidis, A. Molineu, J. R. Palta, C. R. Ramsey, B. J. Salter, et al. IMRT commissioning: multiple institution planning and dosimetry comparisons, a report from AAPM task group 119. *Medical Physics*, 36(11):5359–5373, 2009.

[8] H. Mahmoudzadeh, T. G. Purdie, and T. C. Chan. Constraint generation methods for robust optimization in radiation therapy. *Operations Research for Health Care*, 8:85–90, 2016.

[9] A. Matsuda, T. Matsuda, A. Shibata, K. Katanoda, T. Sobue, H. Nishimoto, and T. J. C. S. R. Group. Cancer incidence and incidence rates in japan in 2008: A study of 25 population-based cancer registries for the monitoring of cancer incidence in japan (MCIJ) project. *Japanese Journal of Clinical Oncology*, 44(4):388–396, 2013.

[10] M. Merritt, Y. Zhang, H. Liu, and R. Mohan. A successive linear programming approach to IMRT optimization problem. Technical Report 41, Dept. of Computational and Applied Mathematics Rice University Patients, 2002.

[11] Ministory of Health, Labour and Welfare. On countmeasures against cancers (in Japanese). `http://www.mhlw.go.jp/stf/shingi/2r9852000001sp25-att/2r9852000001spdf.pdf`. [Online; accessed 25-April-2016].

[12] S. M. Morrill, R. G. Lane, J. A. Wong, and I. I. Rosen. Dose-volume considerations with linear programming optimization. *Medical Physics*, 18(6):1201–1210, 1991.

[13] National Cancer Institute. Radiation therapy for cancer. http://www.cancer.gov/about-cancer/treatment/types/radiation-therapy/radiation-fact-sheet. [Online; accessed 25-April-2016].

[14] P. M. Pardalos and H. E. Romeijn. *Handbook of optimization in medicine*, volume 5. Springer Science & Business Media, 2009.

[15] H. E. Romeijn, R. K. Ahuja, J. F. Dempsey, and A. Kumar. A new linear programming approach to radiation therapy treatment planning problems. *Operations Research*, 54(2):201–216, 2006.

[16] H. E. Romeijn, R. K. Ahuja, J. F. Dempsey, A. Kumar, and J. G. Li. A novel linear programming approach to fluence map optimization for intensity modulated radiation therapy treatment planning. *Physics in Medicine and Biology*, 48(21):3521, 2003.

[17] A. T. Tuncel, F. Preciado, R. L. Rardin, M. Langer, and J. P. P. Richard. Strong valid inequalities for fluence map optimization problem under dose-volume restrictions. *Annals of Operations Research*, 196(1):819–840, 2012.

[18] Q. Wu and R. Mohan. Multiple local minima in IMRT optimization based on dose–volume criteria. *Medical Physics*, 29(7):1514–1527, 2002.